Vol 18 No 5, May 2009
1674-1056/2009/18(05)/1792-09

Chinese Physics B

© 2009 Chin. Phys. Soc.
and IOP Publishing Ltd

Circuit implementation and multiform intermittency in a hyper-chaotic model extended from the Lorenz system*

Cang Shi-Jian(仓诗建)[a)b)†], Chen Zeng-Qiang(陈增强)[b)], and Wu Wen-Juan(吴文娟)[b)]

[a)] *Department of Industry Design, Tianjin University of Science and Technology, Tianjin* 300222, *China*

[b)] *Department of Automation, Nankai University, Tianjin* 300071, *China*

(Received 25 August 2008; revised manuscript received 26 November 2008)

This paper presents a non-autonomous hyper-chaotic system, which is formed by adding a periodic driving signal to a four-dimensional chaotic model extended from the Lorenz system. The resulting non-autonomous hyper-chaotic system can display any dynamic behaviour among the periodic orbits, intermittency, chaos and hyper-chaos by controlling the frequency of the periodic signal. The phenomenon has been well demonstrated by numerical simulations, bifurcation analysis and electronic circuit realization. Moreover, the system is concrete evidence for the presence of Pomeau–Manneville Type-I intermittency and crisis-induced intermittency. The emergence of a different type of intermittency is similarly subjected to the frequency of periodic forcing. By statistical analysis, power scaling laws consisting in different intermittency are obtained for the lifetime in the laminar state between burst states.

Keywords: chaos, circuit implementation, type-I intermittency, crisis-induced intermittency
PACC: 0545, 2960C, 8222D

1. Introduction

Chaos and hyper-chaos have been studied in many aspects, such as nonlinear circuits,[1,2] communication applications,[3] control and synchronization.[4−6] Hyper-chaos exists only in autonomous systems higher than or equal to four-dimensional. In general, hyper-chaos is more disordered than ordinary chaos, and hyper-chaotic systems have more complicated topological structures and dynamics than ordinary chaotic ones. Recently, hyper-chaos has attracted increasing attention from various scientific and engineering communities. These hyper-chaos systems, generally, include rich bifurcation phenomena, such as periodic orbits, tori, intermittency and chaos. Since intermittent phenomena were observed in a variety of real settings and a vast number of numerical models, intermittency has recently become an important research topic.

Because of the chaotic dynamical behaviour, interpreted by theory and observed in practice, a simple system may exhibit many exceptional phenomena such as aperiodic switching between laminar states and chaotic bursts of oscillation. Sustained alternation between these two distinct states is called intermittency. Previous results have accounted for the existence of several different styles of intermittency including Pomeau–Manneville (Type-I, II and III) intermittency[7,8] and crisis intermittency,[9,10] which have their own signatures and scaling. The theory of intermittency, when applied in practice, can help us to better understand some abnormal phenomena, such as the variability of solar and stellar systems in astronomy,[11] the motion of excitable brain cells and of neuronal firing in neuroscience,[12] driven electrohydrodynamic convection in nematics,[13] and so on. Therefore, it is very important to study intermittency performance.

A well-known route from stable orbits to a chaotic state or from one chaotic state to another one (or vice versa) is intermittency which is characterized by the appearance of intermittent short chaotic bursts between quite long quasi-regular (laminar) periods[14] or weakly chaotic laminar phases that are randomly in-

*Project supported in part by the National Natural Science Foundation of China (Grant Nos 60774088 and 10772135), the Program for New Century Excellent Talents in University of China (NCET), the Foundation of the Application Base and Frontier Technology Research Project of Tianjin of China (Grant No 08JCZDJC21900), and the Science and Technology Research Key Project of Education Ministry of China (Grant No 107024).

†Corresponding author. E-mail: csj98231@tust.edu.cn

terrupted by strongly chaotic bursts. The possibility of Pomeau–Manneville intermittency and crisis-induced intermittency may arise when varying a parameter in a dynamical system with a chaotic attractor, which can lose or gain stability.[15]

Pomeau–Manneville intermittency is characterized by a periodic (laminar) phase interrupted by bursts of aperiodic behaviour. This type of intermittency occurs near a tangent bifurcation as the system driving parameter is reduced by a parameter ε from the threshold value for a periodic window. The local Poincaré map of Type I intermittency is $y_{n+1} = y_n + ay_n^2 + \varepsilon(a, \varepsilon > 0)$.[7] The characteristic relation of this type of intermittency is $< l > \propto \varepsilon^{-1/2}$, where $< l >$ is the average laminar length and the channel width between the diagonal and the local Poincaré map. Changes in chaotic attractors with parameter variation, caused by the collision of chaotic attractors with stable manifold and unstable manifold, have been called crises. Crises can be generated by two or more chaotic attractors merging into one chaotic attractor (attractor merging crisis) or a chaotic attractor increasing suddenly in size (interior crisis). Via interior crisis and attractor merging crisis, we have characteristic temporal behaviour that has been named 'crisis-induced intermittency'.

Type-I intermittency and crisis-induced intermittency have been observed in a host of experimental settings.[8,14,16,17] However, an experimental setting with multiform intermittency is unusual. In this paper, we expound concrete evidence for the occurrence of two types of intermittency, namely crisis-induced intermittency and type-I intermittency, in a non-autonomous hyper-chaotic circuit system. Applying a hyper-chaotic system to investigate the phenomenon of these types of intermittency driven by temporal chaos is our aim. The paper is organized as follows. In Section 2, we briefly introduce the non-autonomous hyper-chaotic system. In Sections 3 and 4, several simulations are carried out to give a clear observation on the new chaotic attractor and also some bifurcation analysis. Section 5 introduces the implementation of the hyper-chaotic system via an electronic circuit. Section 6 summarizes our evidence demonstrating the presence of the crisis-induced intermittency and type-I intermittency, and finally in Section 7, we will draw our conclusions.

2. Generating hyper-chaos via a periodic driving signal

We know that, in order to obtain hyper-chaos, two important requisites are as follows:

(i) The minimal dimensions of the phase space in which a hyper-chaotic attractor is embedded should be at least four, because the minimum number of coupled first-order autonomous ordinary differential equations is required to be four.

(ii) The number of terms in the coupled equations giving rise to instability should be at least two, of which at least one should have a nonlinear function.[18]

According to the above two rules, many hyper-chaos systems have been found and constructed. Hyper-chaotic Rössler systems[18] and hyper-chaotic Chua's circuits[19] are two well-known examples. However, there exist many new hyper-chaos systems,[20,21] which are based on the Lorenz chaotic system. By introducing a simple quadratic dynamic feedback control term to the second equation of the Lorenz system, the following four-dimensional dynamic system is obtained.

$$\begin{aligned} \dot{x} &= 10(y - x), \\ \dot{y} &= 28x + y - xz - u, \\ \dot{z} &= xy - \frac{8}{3}z, \\ \dot{u} &= kyz, \end{aligned} \tag{1}$$

where k is a constant for determining the chaotic attractor and bifurcations of the new system.[20] If the feedback control term u equals zero, obviously, the system is a Lorenz chaotic system. When parameter k varies, the hyper-chaotic attractor, chaotic attractor and periodic orbits will occur for different parameters.

Consider the circuit implementation; generally, varying parameter k is realized by controlling the off-the-shelf linear rheostat in size. By this method, however, it is hard to control the parameter k and obtain the bifurcation phenomenon accurately. In order to smooth away the disadvantage in the experiment, a new hyper-chaotic system is proposed by adding a periodic drive signal to the fourth channel of this system.[22] The structure chart of the new system in experiment is demonstrated in Fig.1. For detailed ex-

planation of Fig.1, see Section 5.

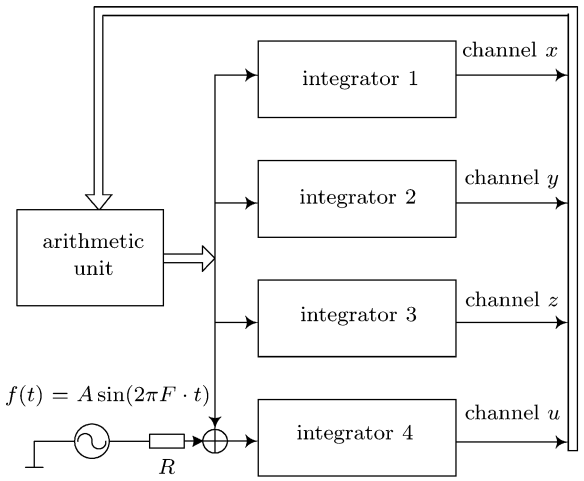


Fig.1. Schematic diagram of the new hyper-chaotic system in circuitry realization.

The four-dimensional non-autonomous dynamic system mentioned above can be described by the following first-order differential equations:

$$\begin{aligned}\dot{x} &= 10(y-x),\\ \dot{y} &= 28x + y - xz - u,\\ \dot{z} &= xy - \frac{8}{3}z,\\ \dot{u} &= kyz + a\sin(\omega t).\end{aligned} \tag{2}$$

If $k = 0.01$ and $a = 500$, via numerical simulation and statistical analysis based on system (2), a rich variety of bifurcation phenomena and new chaotic attractors can be obtained when we control the frequency of the sinusoidal voltage source in the new four-dimensional non-autonomous system.

3. Observation of new chaotic attractors

In system (2), when we adjust the frequency parameter ω of the periodic driving signal, several simulations have been carried out. The outcomes for chaotic attractors and period-doubling bifurcations are summarized as follows:

When $\omega = 1$, there exists a periodic orbit with eight periods, as shown in Fig.2(a);

When $\omega = 2.75$, system (2) enters into chaos motion and the chaotic attractor is shown in Fig.2(b);

When $\omega = 4.34$, system (2) enters into hyper-chaos motion from chaos motion, and the hyper-chaotic attractor is shown in Fig.2(c). Obviously, the attractor shown in Fig.2(c) is different from the one shown in Fig.2(b);

When $\omega = 7.21$, system (2) enters into a periodic orbit with single period again, as shown in Fig.2(d);

When $\omega = 9$, a new chaotic attractor occurs, as shown in Fig.2(e).

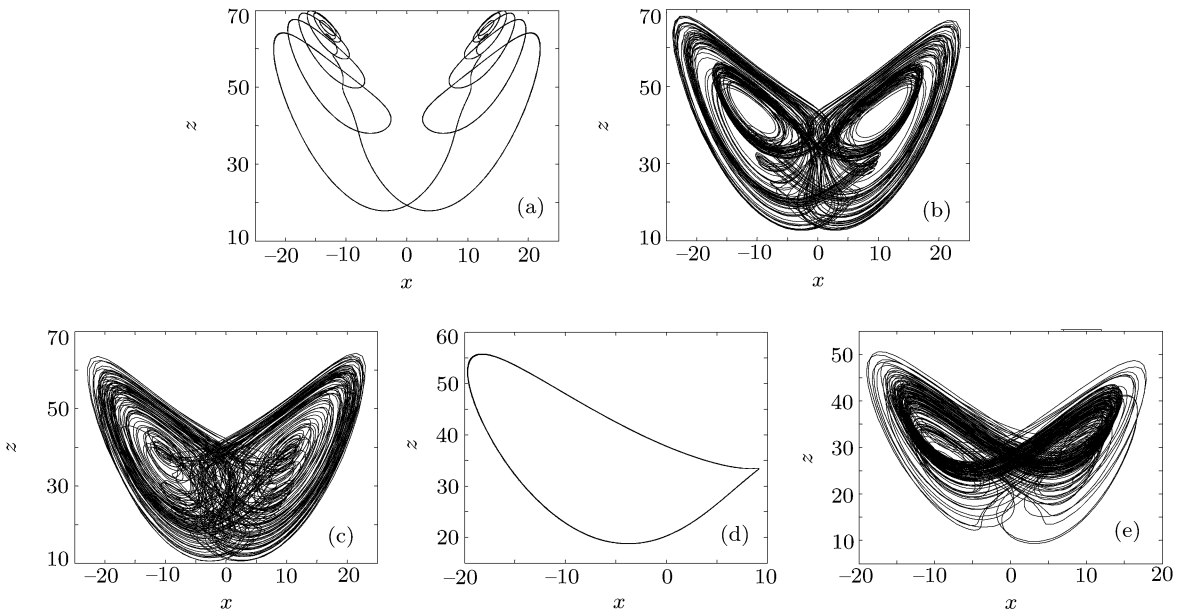


Fig.2. Phase portraits of chaotic system (2) versus increasing frequency ω projected on the $x-z$ plane: (a) $\omega = 1$, periodic orbit; (b) $\omega = 2.75$, chaos; (c) $\omega = 4.34$, hyper-chaos; (d) $\omega = 7.21$, periodic orbit; (e) $\omega = 9$, chaos.

It can be seen from the simulation results that the system undergoes hyper-chaos, chaos, and some different periodic orbits when the frequency varies.

4. Bifurcation analysis

There does not seem to be any systematic methodology for purposefully designing a hyper-chaotic system to date. Therefore, the investigation relies on a combination of mathematical analysis and numerical simulations. As for a hyper-chaotic system, we know that it has distinct features in its Lyapunov exponent. If we assume that the Lyapunov exponents of system (2) are $\lambda_1,\ \lambda_2,\ \lambda_3,\ \lambda_4$ and λ_5, then calculate, we will find that system (2) enters into different states under the condition of some typical different parameter values, as shown in Table 1.

Table 1. Some typical values of ω that lead to different system portraits.

ω	λ_1	λ_2	λ_3	λ_4	λ_5	state
1.00	–0.135	–1.130	–1.962	–8.439	0	periodic orbit
2.75	0.201	–0.035	–2.223	–9.610	0	chaos
4.34	0.418	0.104	–2.099	–10.09	0	hyper-chaos
7.21	–0.194	–0.561	–0.562	–10.25	0	periodic orbit
9.00	0.815	–0.058	–2.157	–10.267	0	chaos

From the bifurcation diagram of state variable x versus parameter ω, we can also find the change between periodic orbits and chaos, as shown in Fig.3.

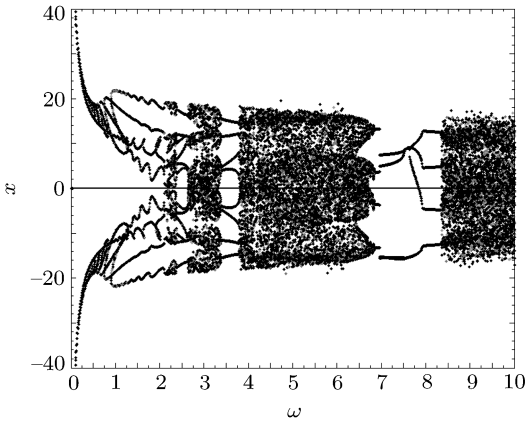


Fig.3. Bifurcation diagram for increasing ω.

5. Circuit implementation and experimental results

According to the structure chart of system (2) mentioned in Section 2, we have designed a circuit implementation for the experimental research. The arithmetic unit in Fig.1 performs the basic operations of addition, subtraction and multiplication of state variables $x,\ y,\ z,\ u$. Integrators $1-4$ perform integration of different channels. Signal $f(t)$ in Fig.1 as a periodic driving signal is added to channel u. The designed circuitry for realizing system (2) is shown in Fig.4.

The operational amplifiers LF347 and associated circuitry perform the basic operations of addition, subtraction, and integration. The nonlinear terms of system (2) are implemented with the analogue multipliers AD633.

A sinusoidal driving signal is derived by function generator YB1638. The input voltage of the sinusoidal driving signal is 2V and is kept unchanged. When we adjust the frequency f of function generator YB1638, rich bifurcation phenomena will emerge in the analogue oscilloscope.

The bifurcation processes of periodic orbits, intermittency, chaos and hyper-chaos can be obtained by simply changing the frequency f of YB1638, and the corresponding attractors and periodic orbits are shown in Figs.5(a)–5(e). As compared with Figs.2(a)–2(e), good qualitative agreement between the numerical simulation and the experimental data is confirmed.

In Figs.5(a)–5(e), the scales of horizontal and vertical axes are 0.5V/div and 2V/div, respectively. All results were recorded from an YB4360 analogue oscilloscope.

Note that the experimental results given above are not exactly the same as the numerical results even if the parameters may be taken as having the same values, as commonly experienced in many case studies between numerical simulations and laboratory experiments. As a matter of fact, the chaos pattern is also sensitive to tiny changes in initial conditions (or during the evolution), and modelling errors and environmental noise are unavoidable in hardware experiments.

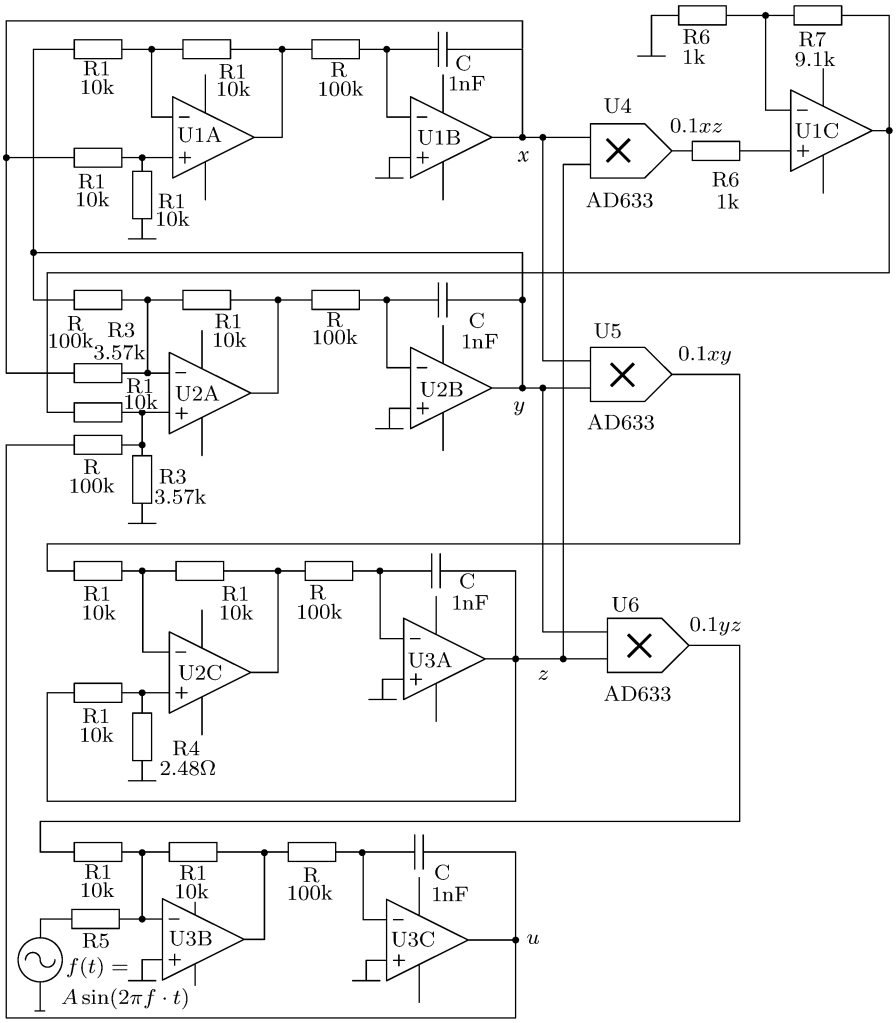


Fig.4. Circuitry realization of the hyper-chaotic system (2).

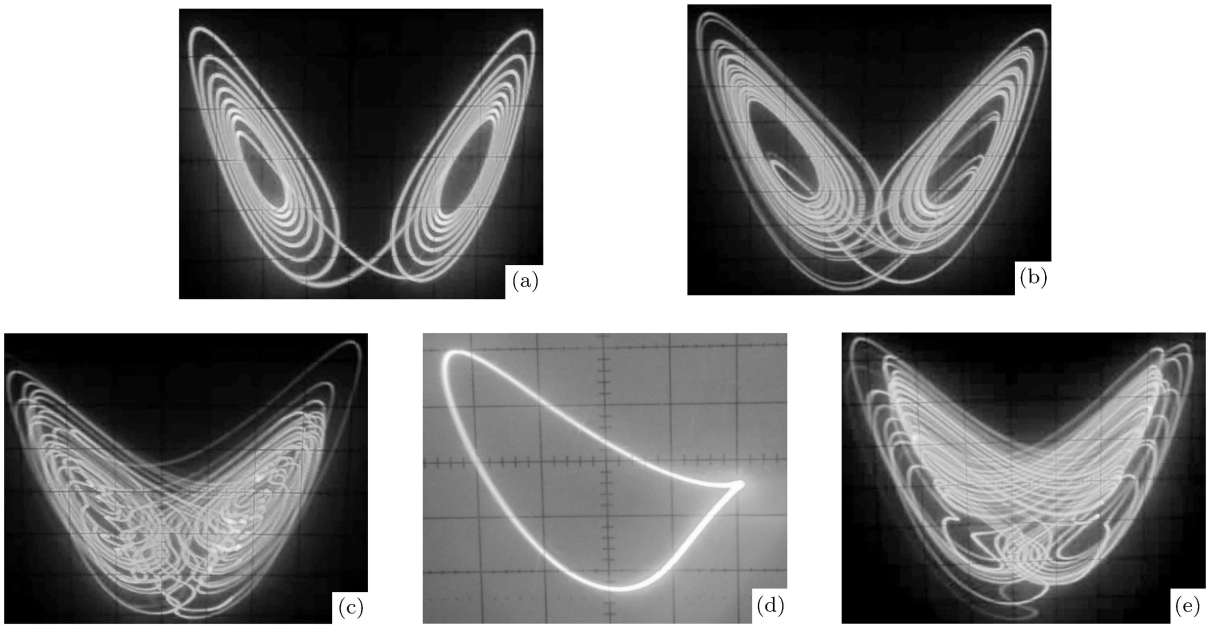


Fig.5. Phase portraits of the system (2) in the $x--z$ plane vs increasing frequency f of function generator YB1638, measured from the experimental setup: (a) $f = 185\,\text{Hz}$, period orbit; (b) $f = 455\,\text{Hz}$, chaotic attractors; (c) $f = 722\,\text{Hz}$, hyper-chaotic attractors; (d) $f = 1.21\,\text{kHz}$, period orbit; (e) $f = 1.47\,\text{kHz}$, chaotic attractors, where the output frequency f is the actual value of function generator YB1638.

6. Intermittency analysis and discussion

Furthermore, if we enlarge the interval [6.1, 8.5] and redraw the bifurcation diagram based on channel x by computer, multiple forms of the intermittency phenomenon will be found by varying the frequency ω. The bifurcation diagram of channel x is shown in Fig.6.

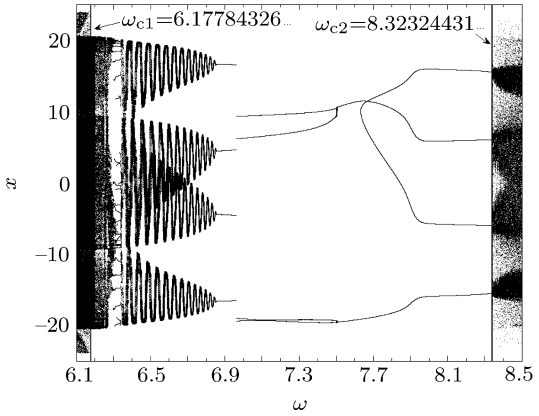


Fig.6. Bifurcation diagram for increasing ω in intervals [6.1, 8.5].

From the bifurcation diagram shown in Fig.6, we can clearly see that a sudden change emerges in the bifurcation diagram when frequency $\omega_{c1} = 6.17784326...$ and $\omega_{c2} = 8.32324431....$ Two critical values are emphasized which we will discuss as follows. In the lower neighbourhood area of frequency $\omega_{c1} = 6.17784326...$, crisis-induced intermittency will occur, while in the higher neighbourhood area of frequency $\omega_{c2} = 8.32324431...$, Pomeau–Manneville Type-I intermittency will emerge.

6.1. Pomeau–Manneville Type-I intermittency

Pomeau–Manneville intermittency including three types of intermittency is characterized by time series containing nearly periodic laminar phases which are interrupted by sudden irregular bursts of chaotic behaviour.[7] Type-I intermittency is brought about when a dynamic system is close to a tangent bifurcation arising from the coalescence of stable and unstable manifolds. There is both experimental and numerical evidence for this intermittency studied extensively in previous work.[23−25] In order to demonstrate the existence of Type-I intermittency in system (2), we have to check, by the plot of the time series, the scaling of the average lifetime between bursts and the power spectrum.

A better way to see the feature of Type-I intermittency in system (2) is to plot with the time series data. When parameter $\omega = 8.323245$, we can obtain the time series of channel x, as shown in Fig.7. From Fig.7, we can see that laminar states are interrupted by burst states randomly, and the duration of laminar states between neighbouring burst states is uncertain. This is a typical feature of intermittency.

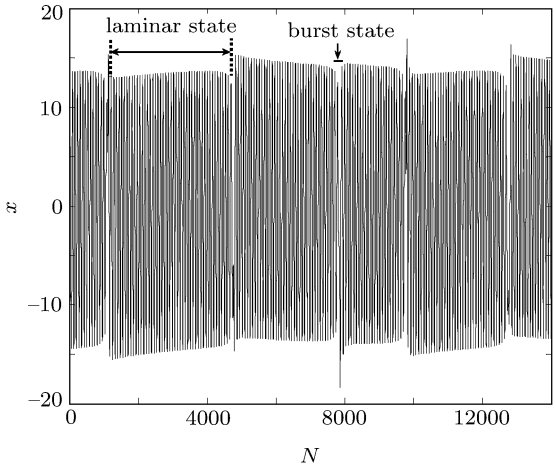


Fig.7. Time series of system (2) with ω=8.323245.

Generally, the duration of one laminar state cannot be confirmed, but we can make sure that the average lifetime of more laminar states is subjected to a correlative parameter. In system (2), the parameter ω is the frequency of the periodic driving signal which determines the average lifetime. For Type-I intermittency, the scaling time of the average lifetime $\langle l \rangle$ between bursts is given by

$$\langle l \rangle \propto (\omega - \omega_{c2})^{-r}, \tag{3}$$

where parameter $r = 0.5$. The scaling factor $r = 0.5$ is an important criterion to distinguish Type-I intermittency from other types of intermittency. By adjusting the frequency ω and $(\omega - \omega_{c2})$ to make it slightly positive, we may obtain Fig.8.

In this case, the critical frequency $\omega_{c2} = 8.32324431....$ By the least squares method, we obtain the slope of numerical calculations shown in Fig.8, which represents the scaling factor. The linear fitting indicated by the continuous line yields a critical exponent $r = 0.47 \approx 0.5$ in Eq.(3).

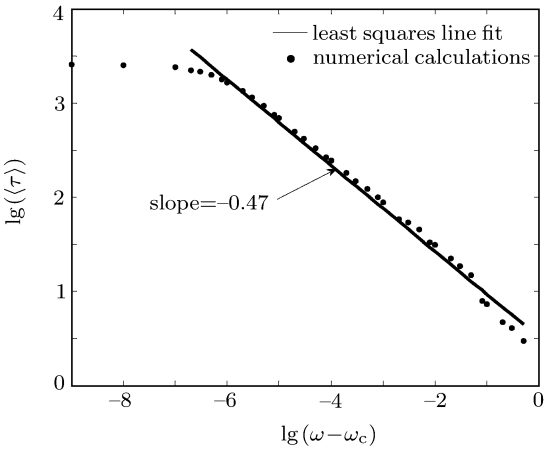


Fig.8. Scaling of the average lifetimes on the parameter $(\omega - \omega_{c2})$.

Another feature of this intermittency is the corresponding power spectrum, since the power spectrum of chaos signal is continuous and the bandwidth is finite. If we define f_s as the saturation frequency, then below or above this frequency there exists a different feature. Below f_s, there is a plateau induced by noise that causes arbitrarily long laminar phases to become finite.[14] Above f_s, the shape of the power spectrum obeys approximately the $1/f$ power law scaling. The power spectrum of the time series with $\omega = 8.323245$ is shown in Fig.9.

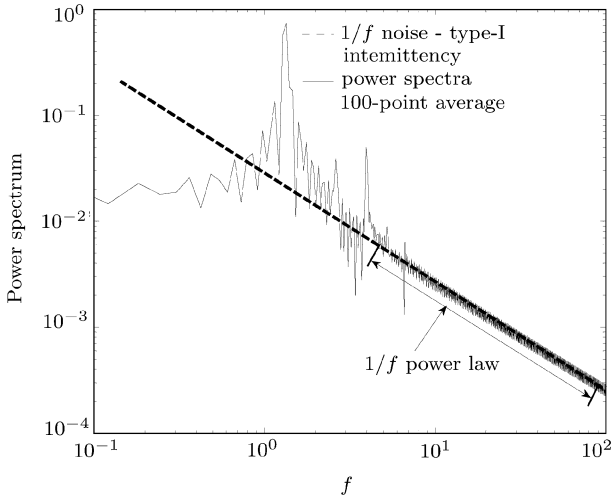


Fig.9. Pwoer spectra of the time series with $\omega = 8.323245$ for type-I intermittency.

6.2. Crisis-induced intermittency

Crisis-induced intermittency is characterized by time series containing weakly chaotic laminar state that are randomly interrupted by strongly chaotic burst states.[8] Crisis-induced intermittency comes in two types of crisis: interior crisis and attractor merging crisis. Here, we are concerned with interior crisis.

For interior crisis in system (2), as parameter ω decreases through ω_{c1}, the chaotic attractor suddenly widens. When ω is slightly smaller than ω_{c1}, the orbit on the attractor spends a long stretch of time in the region to which the attractors were confined before the crisis. At the end of the long stretch the orbit bursts out of the old region and enters chaotically the new enlarged region. It then returns to the old region for another stretch of time again. Figures 10(a) and 10(b) show the time series of system (2) with $\omega = 6.2$ and $\omega = 6.14$, respectively.

We can easily see the weakly chaotic laminar states randomly interrupted by strongly chaotic burst states of the enlarged region by comparing Figs.10(a) and 10(b). The interior crisis occurs when a dynamical system is near a crisis point ($\omega_{c1} = 6.17784326...$), where the weak chaotic attractor collides with strong chaotic attractors.

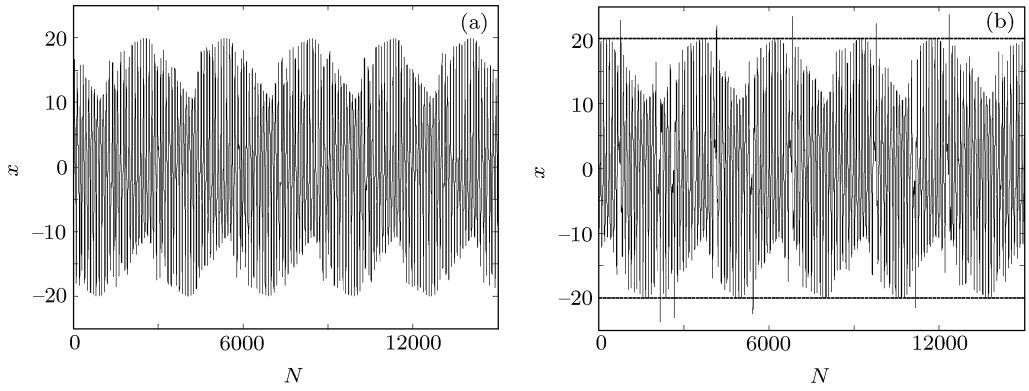


Fig.10. Time series of system (2): (a) $\omega = 6.2$, (b) $\omega = 6.14$.

Figure 11(a) shows a weak attractor just above the crisis point; Fig.11(b) shows a strong attractor just below the crisis point and Fig.11(c) shows superposed two attractors of Figs.11(a) and 11(b). It can be seen from Figs.11(a), 11(b) and 11(c) that the crisis-induced intermittency consists of long intervals of chaotic motion near pre-crisis broken by brief excursions into extended regions of the post-crisis attractors added by the crisis.

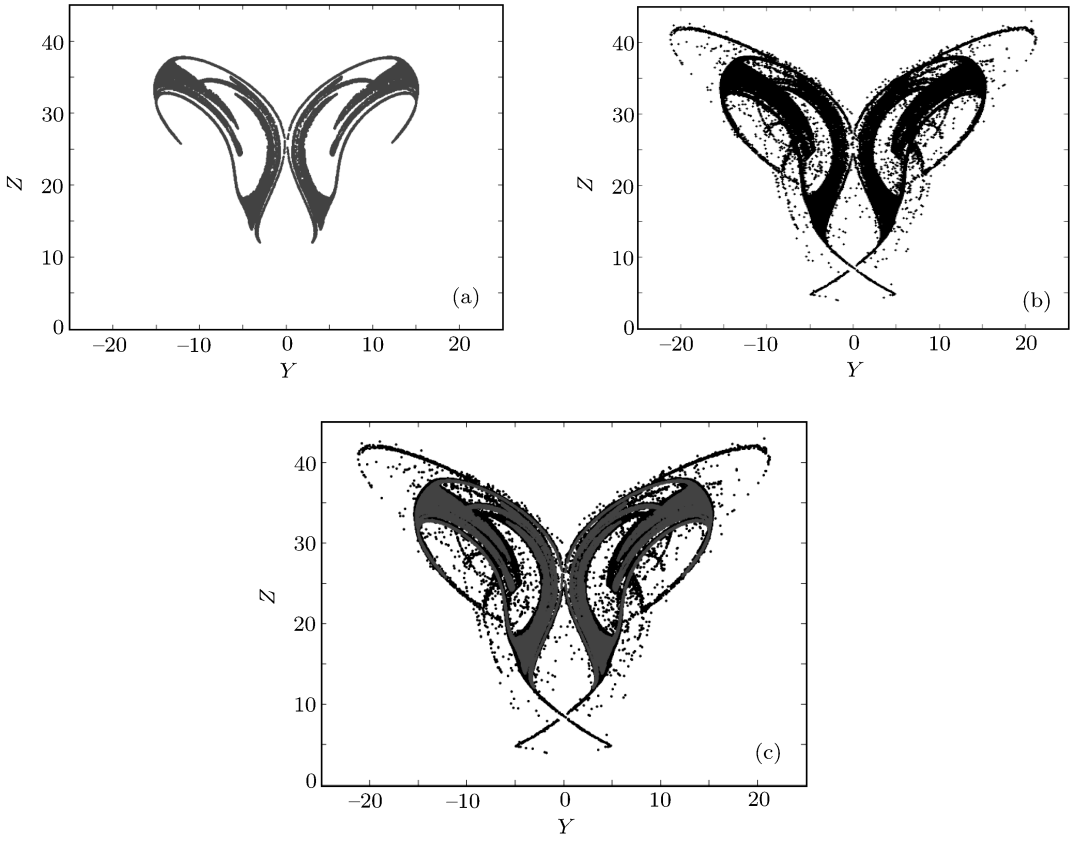


Fig.11. Poincaré section of the crisis-induced intermittency (a): $\omega = 6.2$ (pre-crisis), (b): $\omega = 6.14$ (post-crisis), (c): a superposition of (a) and (b).

The crisis-induced intermittency dynamical system, it is characterized by the lifetime between burst states. The lifetime that the system stays on the pre-crisis attractor has an exponential probability distribution and the average lifetime $\langle\tau\rangle$ obeys a power scaling law[26]

$$\langle\tau\rangle \propto (\omega_{c1} - \omega)^{-r}. \tag{4}$$

When the frequency ω is close to the critical value ω_{c1}, the approximate result $\langle\tau\rangle$ and $(\omega_{c1} - \omega)$ can be obtained. Figure 12 shows the results from numerical experiments determining the average lifetime $\langle\tau\rangle$ as a function of $(\omega_{c1} - \omega)$. We see that a log-log plot of these data is fairly well fitted by a straight line in light of a power law. The slope of the straight line gives $r \cong 1.317$.

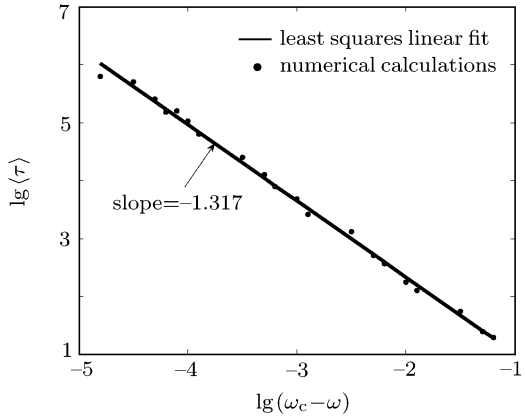


Fig.12. The average lifetime versus the parameter $(\omega_{c1} - \omega)$ in a logarithm plot.

7. Conclusion

By adding a periodic driving signal to a four-dimensional chaotic model extended from the Lorenz system, a new hyper-chaotic system will be obtained. The resulting non-autonomous hyper-chaotic system with a particular parameter, which can be adjusted shrewdly and accurately by controlling the frequency of the periodic signal, has any dynamic behaviour among the periodic orbits, intermittency, chaos and hyper-chaos. These phenomena have been well demonstrated by numerical simulations, bifurcation analysis and electronic circuit realization. According to the bifurcation analysis, we further find the existence of Pomeau–Manneville Type-I intermittency and crisis-induced intermittency. The emergence of multiple forms of intermittency is subject to the frequency of periodic forcing. Furthermore, statistical analysis helps us to gain the power scaling laws of different intermittency for the lifetimes of laminar states and between burst states, respectively. In terms of the signature of the bifurcation diagram, spectra and power scaling law, the existence of Pomeau–Manneville Type-I intermittency and crisis-induced intermittency is demonstrated thoroughly and systematically.

References

[1] Cafagna D and Grassi G 2003 *Int. J. Bifur. Chaos* **13** 2889
[2] Liu C X 2002 *Acta Phys. Sin.* **51** 1198 (in Chinese)
[3] Li W L and Song Y Z 2008 *Acta Phys. Sin.* **57** 51 (in Chinese)
[4] Yassen M 2006 *Phys. Lett.* A **350** 36
[5] Liu C X 2007 *Chin. Phys.* **16** 3279
[6] Song Y Z, Zhao G Z and Qi D L 2006 *Chin. Phys.* **15** 2266
[7] Pomeau Y and Manneville P 1980 *Commun. Math. Phys.* **74** 189
[8] Wang W H, He Y X, Gao Z, Zeng L, Zhang G P, Xie L F and Feng C H 2004 *Chin. Phys.* **13** 2091
[9] Grebogi C, Ott E and Yorke J 1983 *Physica* D **7** 181
[10] Grebogi C, Ott E, Romerias F and Yorke J 1987 *Phys. Rev.* A **36** 5365
[11] Tavakol R and Covas E 1999 arXiv:astro-ph/9904394v1
[12] Korn H and Faure P 2003 *C.R. Biologies* **326** 787
[13] John T, Stannarius R and Behn U 1999 *Phys. Rev. Lett.* **83** 749
[14] Covas E and Tavakol R 1999 *Phys. Rve.* E **60** 5435
[15] Jeffries C and Perez J 1982 *Phys. Rev.* A **26** 2117
[16] Manffra E, Caldas I, Viana R and Kalinowski H 2002 *Nonlinear Dynam.* **27** 185
[17] Zhou Q, Chen Z Q and Yuan Z Z 2007 *Chin. Phys.* **16** 2616
[18] Rössler E O 1979 *Phys. Lett.* A **71** 155
[19] Brucoli M, Carnimeo L and Grassi L 1996 *Int. J. Bifur. Chaos* **6** 1673
[20] Liu C X 2007 *Acta Phys. Sin.* **56** 6865 (in Chinese)
[21] Wang X Y and Wang M J 2007 *Acta Phys. Sin.* **56** 5136 (in Chinese)
[22] Cang S J, Chen Z Q and Yuan Z Z 2008 *Acta Phys. Sin.* **57** 1493 (in Chinese)
[23] Arjona M, Pujol J and Corbalán R 1994 *Phys. Rve.* A **50** 871
[24] Kye W and Kim C 2000 *Phys. Rve.* E **62** 6304
[25] Franck C, Klinger T and Piel A 1999 *Phys. Lett.* A **259** 152
[26] Kacperski K and Holyst J 1999 *Phys. Rev.* E **60** 403